ADVANCED HEALTHCARE MATERIALS
www.advhealthmat.com

Fluorescent 2D WS_2 Nanosheets Bearing Chemical Affinity Elements for the Recognition of Glycated Hemoglobin

*Jin-Kyoung Yang, Hye-Rim Lee, In-Jun Hwang, Hye-In Kim, DaBin Yim, and Jong-Ho Kim**

It is required to exfoliate and functionalize 2D transition metal dichalcogenides (TMDs) in an aqueous solution for biological and medical applications. Herein, the approach for the simultaneous exfoliation and functionalization of 2D WS_2 nanosheets using boronic acid-modified poly(vinyl alcohol) (B-PVA) in an aqueous solution is reported, and the B-PVA-functionalized WS_2 nanosheets (B-PVA-WS_2) are exploited as a fluorescent biosensor for the detection of glycated hemoglobin, HbA1c. The synthetic B-PVA polymer facilitates the exfoliation and functionalization of WS_2 nanosheets from the bulk counterpart in the aqueous solution via a pulsed sonication process, resulting in fluorescent B-PVA-WS_2 nanohybrids with a specific recognition of HbA1c. The fluorescence of the B-PVA-WS_2 is quenched in the presence of HbA1c, whereas PVA-functionalized WS_2 (PVA-WS_2), not bearing boronic acid as a recognition moiety, shows no fluorescence changes upon the addition of the target. The B-PVA-WS_2 is able to selectively detect HbA1c at the concentration as low as 3.3×10^{-8} M based on its specific fluorescence quenching.

2D transition metal dichalcogenides (TMDs) have recently attracted considerable attention in diverse research fields due to their unique physicochemical properties that are dependent on chemical composition and physical dimensions.[1–3] In particular, the electronic band structures of TMDs can be tuned from indirect to direct bandgaps by forming monolayer TMDs, resulting in strong fluorescence emission over the visible range.[4,5] To effectively utilize the fluorescence properties of TMDs for biological, medical, and aqueous-phase catalytic applications,[6] aqueous-phase exfoliation and functionalization of TMD monolayers are required. However, aqueous liquid exfoliation requires additives to reduce the surface energy of the TMD monolayers, whereas organic liquid exfoliation requires solvents with a surface tension close to that of TMDs.[7] To date, several strategies have been developed for the exfoliation of thin TMD nanosheets in water using polymers,[8–10] surfactants,[11,12] DNA,[13] and proteins such as bovine serum albumin,[14] lysozyme,[15] and hydrophobin,[16] However, it is still challenging to impart specific functions to fluorescent 2D TMD nanosheets during exfoliation in water. Therefore, it is of great interest to develop an effective method for the simultaneous exfoliation and functionalization of thin TMD nanosheets with strong fluorescence in water.

Glycated hemoglobin (HbA1c) is produced via the glycation of the N-terminal valine groups of hemoglobin in red blood cells, whose life span is 120 d, and reflects the long-term glycemic index in blood.[17–20] HbA1c is a more promising biomarker than plasma glucose for the diagnosis of both type I and type II diabetes and the long-term monitoring of glycemic levels because the concentration of glucose in plasma frequently fluctuates depending on diet, physical activity, and health conditions.[18,19,21] The current gold standard for the detection of HbA1c is a chromatographic method.[22] However, it requires multiple analytical processes, long assay times, and expensive instrumentation. Hence, great effort has been dedicated to the development of biosensors for the simple and rapid detection of HbA1c, including immunoassays,[23–25] electrochemical sensing,[26–29] and optical detection,[30,31] However, demand remains high for new sensing methods enabling the point-of-care of HbA1c with high accuracy and user friendliness.[32] In particular, the design of TMD fluorescence-based biosensors for the detection of HbA1c is of great interest but has not been reported to date.

Herein, we report an effective approach for the simultaneous exfoliation and functionalization of fluorescent 2D WS_2 nanosheets with HbA1c recognition capability in an aqueous solution. Moreover, the performance of the prepared 2D WS_2 nanosheets for HbA1c detection based on their fluorescence quenching was examined (**Figure 1**).

To exfoliate and functionalize WS_2 nanosheets simultaneously in water, boronic acid-modified poly(vinyl alcohol) (B-PVA) was synthesized via esterification between the hydroxyl groups of PVA and the carboxyl group of carboxyphenylboronic acid (CPBA) (**Figure 2**a). The boronic acid moiety acts as a chemical recognition element for HbA1c, because it can form reversible bonds with the *cis*-diol groups of carbohydrates.[33] The obtained B-PVA was characterized by Fourier transform infrared (FT-IR) spectroscopy. The vibrational modes corresponding to an ester carbonyl group (C=O, 1709 cm^{-1}), aromatic sp^2 carbon (C=C, 1400–1600 cm^{-1}), and boronic acid (B—O, 1304 cm^{-1}) were

Dr. J.-K. Yang, H.-R. Lee, I.-J. Hwang, H.-I. Kim, D. Yim, Prof. J.-H. Kim
Department of Chemical Engineering
Hanyang University
Ansan 426-791, Republic of Korea
E-mail: kjh75@hanyang.ac.kr

The ORCID identification number(s) for the author(s) of this article can be found under https://doi.org/10.1002/adhm.201701496.

DOI: 10.1002/adhm.201701496

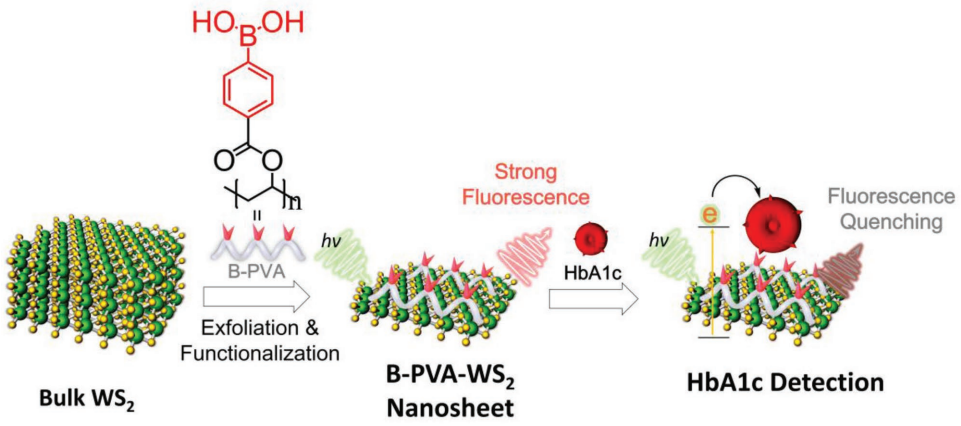

Figure 1. Schematic illustration for the simultaneous exfoliation and functionalization of WS_2 nanosheets with B-PVA and the B-PVA-WS_2 nanosheet-based optical sensor for the selective detection of glycated hemoglobin, HbA1c.

observed in the FT-IR spectrum of B-PVA (Figure 2b). In addition, π–π^* and n–π^* transitions, which are characteristic of the phenyl and carbonyl groups in CPBA, were clearly observed at 236 and 279 nm, respectively, in the absorption spectrum of B-PVA (Figure 2c). This spectroscopic characterization indicated that B-PVA was successfully synthesized. The boronic acid content in B-PVA was then quantified by a calibration curve based on the absorbance of CPBA at 279 nm (Figure S1, Supporting Information). It was found that 1.69 mmol g^{-1} of boronic acid was incorporated into B-PVA.

Next, B-PVA was used for the simultaneous exfoliation and functionalization of thin WS_2 nanosheets in water. Bulk WS_2 was sonicated in the presence of B-PVA in water, and the resulting mixture was centrifuged to obtain B-PVA-functionalized WS_2 (B-PVA-WS_2) nanosheets. The physical and chemical structures of the B-PVA-WS_2 nanosheets were analyzed by transmission electron microscopy (TEM), FT-IR spectroscopy, and X-ray photoelectron spectroscopy (XPS) after the free B-PVA was removed. The TEM image of the B-PVA-WS_2 nanosheets showed a distinct thin 2D structure with a lateral size of ≈50 nm (**Figure 3**a). The lattice structure and selected-area electron diffraction pattern of the B-PVA-WS_2 nanosheets clearly show that they retained an intrinsic 2H phase after exfoliation and functionalization with B-PVA in water (Figure 3b). The chemical structure of the B-PVA-WS_2 nanosheets was confirmed through the observation

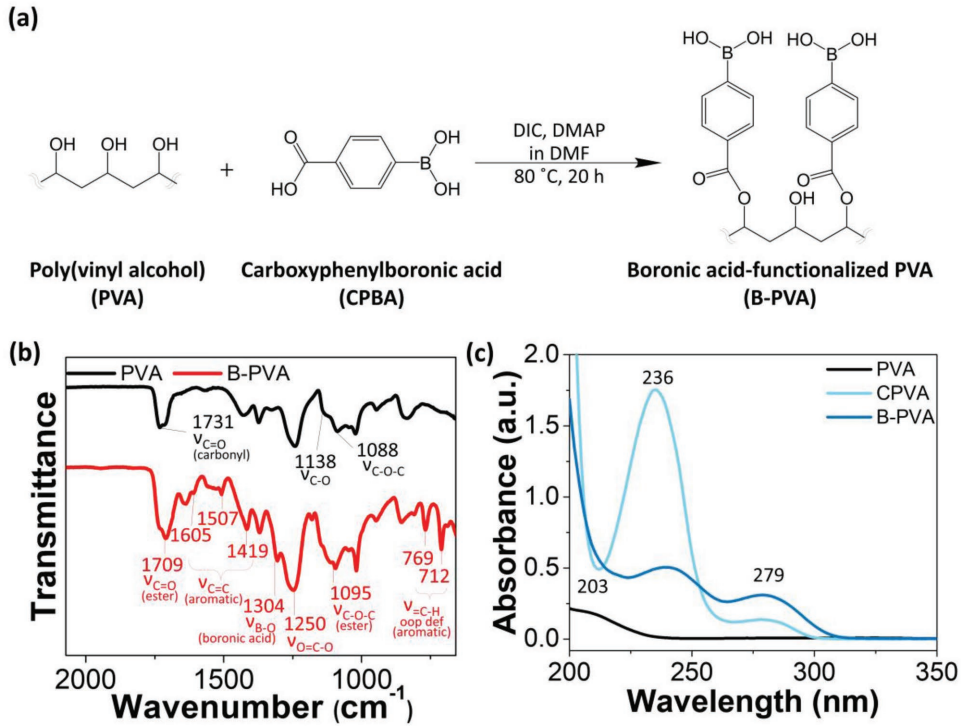

Figure 2. Synthesis of B-PVA. a) Scheme for the synthesis of B-PVA. b) FT-IR spectra of PVA and B-PVA. c) UV–vis spectra of PVA, CPBA, and B-PVA.

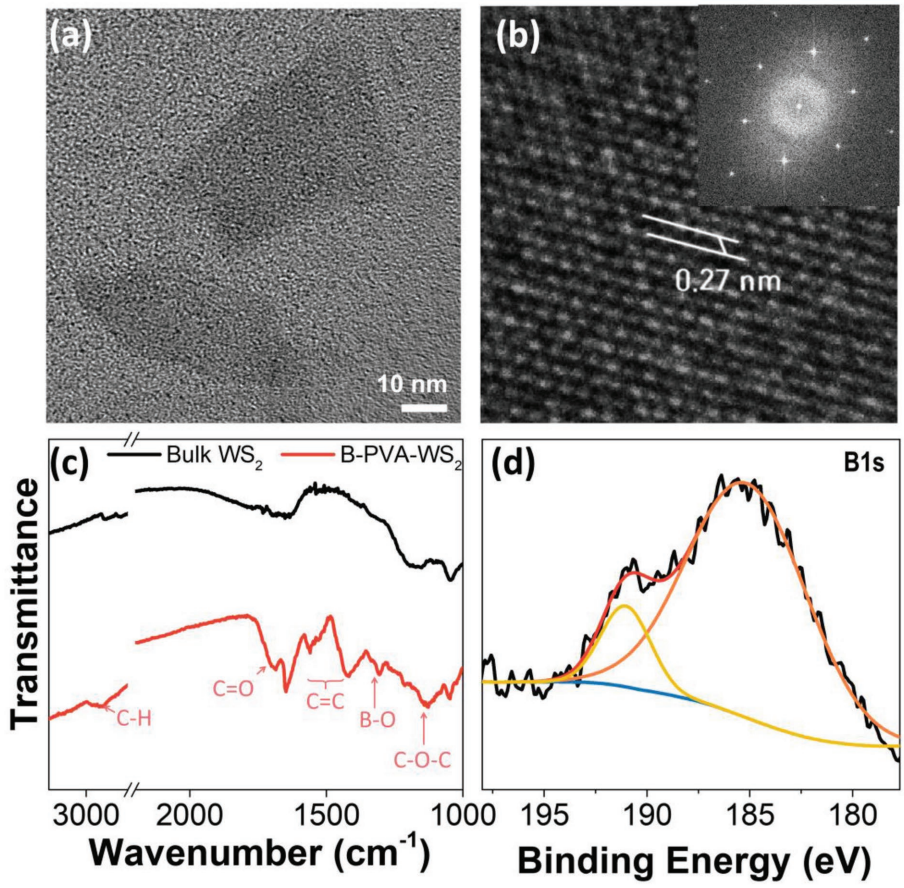

Figure 3. Structural characterization of B-PVA-WS_2 nanosheets. a) Representative TEM image and b) corresponding HRTEM image of B-PVA-WS_2 nanosheets. Inset: FFT pattern. c) FT-IR spectra of bulk WS_2 (black line) and B-PVA-WS_2 nanosheets (red line). d) B1s XPS spectrum of B-PVA-WS_2 nanosheets.

of the vibrational modes of C–H (2928 cm^{-1}), C=O (1693 cm^{-1}), C=C (1400–1600 cm^{-1}), B—O (1306 cm^{-1}), and C—O—C (1124 cm^{-1}) bonds in the FT-IR spectrum (Figure 3c). Furthermore, the characteristic peaks of the C—B—$(OH)_2$ moiety were clearly observed at 191.2 and 185.7 eV in the B1s XPS spectrum of the B-PVA-WS_2 nanosheets (Figure 3d).[34] These results indicate that the surface of the WS_2 nanosheets was successfully functionalized by B-PVA in water.

Subsequently, the optical properties of the B-PVA-WS_2 nanosheets were investigated. As shown in **Figure 4**a, characteristic A1 and B1 excitonic absorptions were clearly observed at 619 and 514 nm, respectively, indicating that thin WS_2 nanosheets with a direct bandgap were produced from its bulk counterpart with an indirect bandgap. Fluorescence is also a good index to assess the effectiveness of the exfoliation process. The B-PVA-WS_2 nanosheets exhibited fluorescence emission at 614 nm under excitation at 532 nm (Figure 4b), indicating effective exfoliation of WS_2 monolayers with a direct bandgap in water. The 532 nm excitation provided the B-PVA-WS_2 nanosheets with the highest fluorescence-to-background ratio without overlapping with the Raman scattering signal of water. These results reveal that the simultaneous exfoliation and functionalization of WS_2 nanosheets with B-PVA in water were achieved.

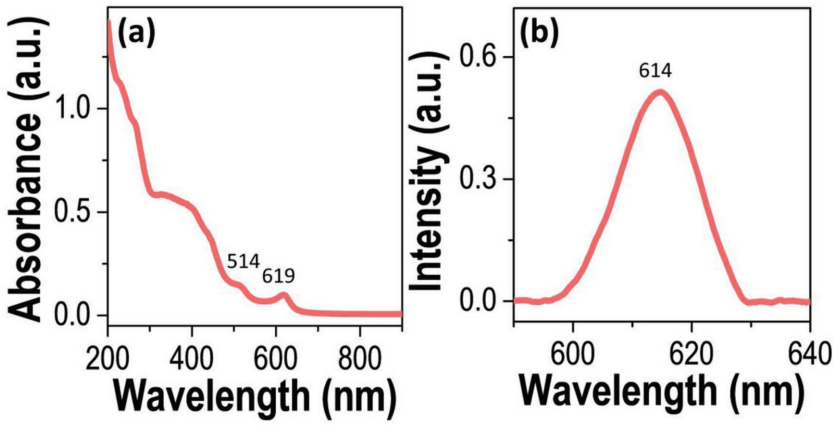

Figure 4. Optical properties of B-PVA-WS_2. a) UV–vis absorption and b) PL spectra of B-PVA-WS_2 under excitation at 532 nm.

The performance of B-PVA-WS_2 for the detection of HbA1c was then evaluated. After addition of HbA1c (3.3×10^{-7} M) to the B-PVA-WS_2 solution, the fluorescence response of the B-PVA-WS_2 sensor was measured over time (Figure S2, Supporting Information). The fluorescence quenching of the B-PVA-WS_2 sensor gradually increased as the reaction time increased until 10 min. However, the fluorescence quenching of the B-PVA-WS_2 sensor did not increase further at reaction time beyond 10 min, indicating that its fluorescence response to HbA1c reached an equilibrated state within 10 min. Different concentrations of HbA1c were incubated with the B-PVA-WS_2 nanosheets in Tris-HCl buffer (pH 8.0) at room temperature (RT) for 10 min, followed by measurement of the fluorescence signal of the B-PVA-WS_2 nanosheets at an excitation wavelength of 532 nm. As shown in **Figure 5**a, the fluorescence of the B-PVA-WS_2 nanosheets gradually diminished as the concentration of HbA1c increased, indicating that they were able to recognize the target HbA1c. This fluorescence quenching is likely caused by charge transfer from the B-PVA-WS_2 nanosheets to the heme group of HbA1c when in close proximity.[35] Fluorescence resonance energy transfer between the B-PVA-WS_2 nanosheets and HbA1c is unlikely to occur because there is no spectral overlapping between the fluorescence emission of the sensor and the absorption of HbA1c.[36] For comparison, WS_2 nanosheets were also exfoliated using pristine PVA (PVA-WS_2), without boronic acid moieties, and their fluorescence in the presence of HbA1c was measured. The as-prepared PVA-WS_2 also exhibited strong fluorescence and characteristic excitonic peaks (Figure S3, Supporting Information). When the PVA-WS_2 was incubated with HbA1c at various concentrations, the fluorescence remained constant (Figure 5b, black line). Conversely, the B-PVA-WS_2 showed a distinct quenching response to HbA1c (Figure 5b, red line). The limit of detection (LOD) of the B-PVA-WS_2 sensor was calculated based on the standard deviation (SD) of the response and the slope of the calibration curve (S) at levels approximating the LOD according to the formula: LOD = 3.3(SD/S).[37–39] After linear fitting of the data, S and SD were found to be 1.207 and 0.012, respectively. Based on these values, LOD of the B-PVA-WS_2 sensor was found to be 3.3×10^{-8} M. These results indicate that the B-PVA functionalization imparts a specific recognition capability to the WS_2 nanosheets.

Finally, the B-PVA-WS_2 nanosheets were applied to the selective detection of HbA1c in the presence of glucose as a potential interfering substance. According to the estimated average glucose (eAG) level established by the National Glycohemoglobin Standardisation Program and International Federation of Clinical Chemistry,[40] the molar ratio of HbA1c with eAG was found to be 1:70 in diabetes patients. Hence, 2.3×10^{-4} M of glucose, which is 70 times higher than the highest

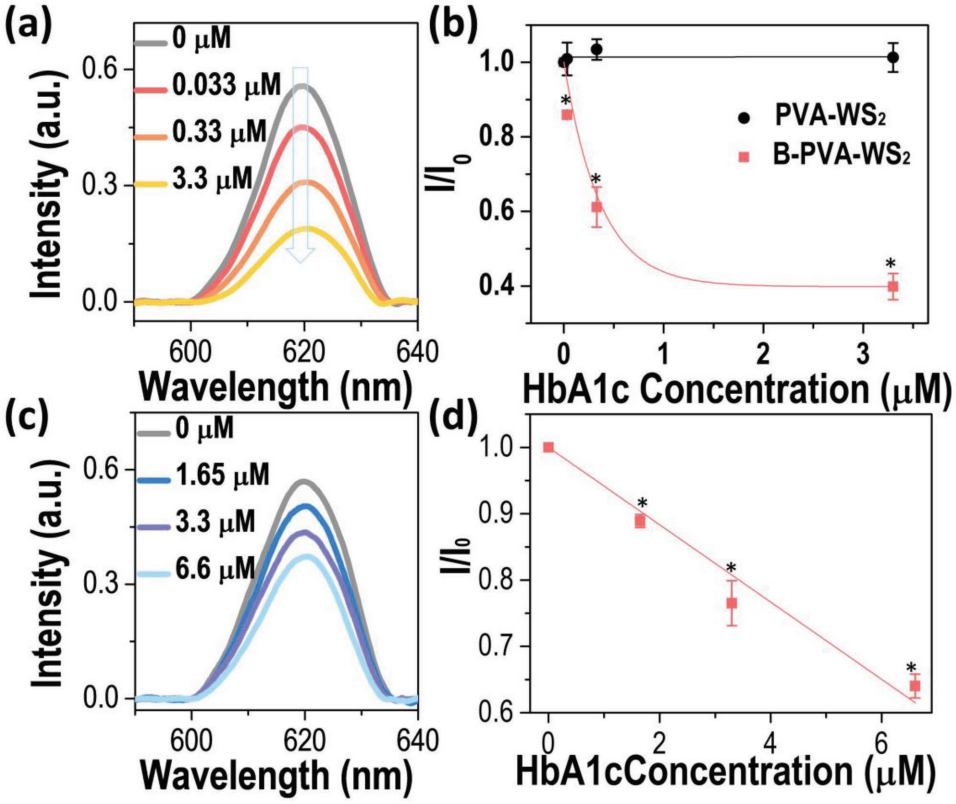

Figure 5. Fluorescent detection of HbA1c using B-PVA-WS_2. a) PL spectra of B-PVA-WS_2 nanosheets achieved by varying the concentration of HbA1c. b) Comparison of PL quenching responses between PVA-WS_2 and B-PVA-WS_2 in the presence of HbA1c. c) Fluorescence spectra and d) fluorescence quenching response of B-PVA-WS_2 nanosheets as a function of HbA1c concentrations in the presence of glucose (2.3×10^{-4} M). I_0 and I are the intensities in the absence and the presence of HbA1c at each concentration (pH 8.0, RT). All spectra were obtained under excitation at 532 nm. The measurement was performed in triplicate and all reported values represent the mean ± SD ($n = 3$). *$p < 0.001$ versus negative control by Student's t-test.

concentration of HbA1c, was added with HbA1c to the B-PVA-WS_2 solution. The fluorescence of the B-PVA-WS_2 nanosheets was linearly quenched even in the presence of a high concentration of glucose (2.3×10^{-4} M, Figure 5c,d) although the extent of the quenching response slightly decreased. This diminished quenching response of the B-PVA-WS_2 sensor might be ascribed to the fact that a high concentration of glucose competes with HbA1c for binding to the boronic acid groups on the sensor. This apparently shows that the constructed B-PVA-WS_2 sensor possesses high selectivity for HbA1c.

In conclusion, we developed an approach for the simultaneous exfoliation and functionalization of 2D WS_2 nanosheets with B-PVA in water. The as-prepared B-PVA-WS_2 nanosheets exhibited fluorescence in the visible range and were capable of selectively, sensitively, and rapidly recognizing HbA1c via their fluorescence quenching. This exfoliation and functionalization strategy can likely be expanded to design various 2D nanomaterials with specific functions. In addition, the sensing principle based on the fluorescence quenching of the B-PVA-WS_2 nanosheets can be applied for the detection of various biological molecules.

Experimental Section

Synthesis of B-PVA: PVA (600 mg) was dissolved in 40 mL of DMF in which CPBA (338 mg) was added. After *N,N′*-diisopropylcarbodiimide (386 mg) and 4-(dimethylamino)pyridine (374 mg) were added to the PVA solution at RT, the mixture was stirred at 80 °C for 20 h. After addition of 40 mL of water to the reaction mixture, the desired product was purified using a 1 kDa cellulose membrane and then dried under vacuum. B-PVA was characterized with UV–vis spectrophotometer, FT-IR spectroscopy, and nuclear magnetic resonance.

Exfoliation of WS_2 Nanosheets with B-PVA (B-PVA-WS_2): Bulk WS_2 (3.6 g) was added to the B-PVA aqueous solution (2 g L^{-1}, 120 mL) in 250 mL of a beaker, followed by sonication at 100 W power with a pulse sequence of 6 s on and 2 s off for 1 h. The resulting dispersion was centrifuged at 2500 g for 90 min to obtain the sediment. The sediment was then redispersed in 120 mL of a fresh B-PVA solution, followed by sonication at 100 W power with a pulse sequence of 6 s on and 2 s off for 5 h. The resulting dispersion was centrifuged at 2500 g for 90 min, and the obtained supernatant was centrifuged again at 10 000 g for 90 min to obtain the sediment. Finally, the sediment was subjected to further centrifugation at 3500 g for 90 min to obtain B-PVA-WS_2.

Fluorescence Detection of HbA1c: The B-PVA-WS_2 solution (90 µg, 300 µL) was added to a 96-well plate. After addition of HbA1c at a certain concentration in Tris-HCl buffer (10×10^{-3} M, pH 8.0), the reaction mixture was incubated for 10 min at RT. The final concentration of HbA1c was varied from 0 to 3.3×10^{-6} M. Then, the fluorescence of the B-PVA-WS_2 was measured under excitation at 532 nm (7.5 mW laser power). For the investigation of selectivity for HbA1c detection, glucose (1.06 mg mL^{-1}) was premixed with HbA1c in Tris-HCl buffer (1.0×10^{-5} M, pH 8.0) at RT, and then the glucose/HbA1c mixture was added to the B-PVA-WS_2 solution.

Statistical Analysis: All the data presented here were obtained from at least three independent experiments ($n \geq 3$), and the values were represented as the mean ± the SD unless indicated otherwise. The probability (P) values were obtained using unpaired two-tailed Student's *t*-test.

Supporting Information

Supporting Information is available from the Wiley Online Library or from the author.

Acknowledgements

J.-K.Y. and H.-R.L. contributed equally to this work. This work was supported by the Basic Science Research Program (2008-0061891, NRF-2014R1A2A1A11051877, and NRF-2017R1A2B2008455) through the National Research Foundation of Korea funded by the Ministry of Science and ICT.

Conflict of Interest

The authors declare no conflict of interest.

Keywords

aqueous exfoliation, fluorescent WS_2 nanosheet, HbA1c detection, optical biosensors, WS_2 functionalization

Received: December 23, 2017
Revised: February 22, 2018
Published online:

[1] Q. H. Wang, K. Kalantar-Zadeh, A. Kis, J. N. Coleman, M. S. Strano, *Nat. Nanotechnol.* **2012**, *7*, 699.
[2] M. Chhowalla, H. S. Shin, G. Eda, L.-J. Li, K. P. Loh, H. Zhang, *Nat. Chem.* **2013**, *5*, 263.
[3] W. Choi, N. Choudhary, G. H. Han, J. Park, D. Akinwande, Y. H. Lee, *Mater. Today* **2017**, *20*, 116.
[4] J. Kang, S. Tongay, J. Zhou, J. Li, J. Wu, *Appl. Phys. Lett.* **2013**, *102*, 012111.
[5] W. J. Zhao, Z. Ghorannevis, L. Q. Chu, M. L. Toh, C. Kloc, P. H. Tan, G. Eda, *ACS Nano* **2013**, *7*, 791.
[6] K. Kalantar-zadeh, J. Z. Ou, T. Daeneke, M. S. Strano, M. Pumera, S. L. Gras, *Adv. Funct. Mater.* **2015**, *25*, 5086.
[7] J. N. Coleman, M. Lotya, A. O'Neill, S. D. Bergin, P. J. King, U. Khan, K. Young, A. Gaucher, S. De, R. J. Smith, I. V. Shvets, S. K. Arora, G. Stanton, H. Y. Kim, K. Lee, G. T. Kim, G. S. Duesberg, T. Hallam, J. J. Boland, J. J. Wang, J. F. Donegan, J. C. Grunlan, G. Moriarty, A. Shmeliov, R. J. Nicholls, J. M. Perkins, E. M. Grieveson, K. Theuwissen, D. W. McComb, P. D. Nellist, V. Nicolosi, *Science* **2011**, *331*, 568.
[8] Y. Yuan, R. Li, Z. Liu, *Anal. Chem.* **2014**, *86*, 3610.
[9] V. Vega-Mayoral, C. Backes, D. Hanlon, U. Khan, Z. Gholamvand, M. O'Brien, G. S. Duesberg, C. Gadermaier, J. N. Coleman, *Adv. Funct. Mater.* **2016**, *26*, 1028.
[10] L. Zong, M. Li, C. Li, *Adv. Mater.* **2017**, *29*, 1604691.
[11] R. J. Smith, P. J. King, M. Lotya, C. Wirtz, U. Khan, S. De, A. O'Neill, G. S. Duesberg, J. C. Grunlan, G. Moriarty, *Adv. Mater.* **2011**, *23*, 3944.
[12] C. Backes, B. M. Szydłowska, A. Harvey, S. Yuan, V. Vega-Mayoral, B. R. Davies, P.-l. Zhao, D. Hanlon, E. J. Santos, M. I. Katsnelson, *ACS Nano* **2016**, *10*, 1589.
[13] G. S. Bang, S. Cho, N. Son, G. W. Shim, B.-K. Cho, S.-Y. Choi, *ACS Appl. Mater. Interfaces* **2016**, *8*, 1943.
[14] G. Guan, S. Zhang, S. Liu, Y. Cai, M. Low, C. P. Teng, I. Y. Phang, Y. Cheng, K. L. Duei, B. M. Srinivasan, *J. Am. Chem. Soc.* **2015**, *137*, 6152.
[15] M. Siepi, E. Morales-Narváez, N. Domingo, D. M. Monti, E. Notomista, A. Merkoçi, *2D Mater.* **2017**, *4*, 035007.
[16] J. Kaur, A. M. Gravagnuolo, P. Maddalena, C. Altucci, P. Giardina, F. Gesuele, *RSC Adv.* **2017**, *7*, 22400.
[17] A. D. Association, *Diabetes Care* **2011**, *34*, S11.

[18] E. Selvin, M. W. Steffes, H. Zhu, K. Matsushita, L. Wagenknecht, J. Pankow, J. Coresh, F. L. Brancati, *N. Engl. J. Med.* **2010**, *2010*, 800.
[19] C. Bennett, M. Guo, S. Dharmage, *Diabetic Med.* **2007**, *24*, 333.
[20] C. Weykamp, *Ann. Lab. Med.* **2013**, *33*, 393.
[21] C. Rohlfing, H.-M. Wiedmeyer, R. Little, V. L. Grotz, A. Tennill, J. England, R. Madsen, D. Goldstein, *Clin. Chem.* **2002**, *48*, 1116.
[22] C.-N. Ou, C. L. Rognerud, *Clin. Chem.* **1993**, *39*, 820.
[23] D.-H. Kuan, I.-S. Wang, J.-R. Lin, C.-H. Yang, C.-H. Huang, Y.-H. Lin, C.-T. Lin, N.-T. Huang, *Lab Chip* **2016**, *16*, 3105.
[24] G. Liu, S. M. Khor, S. G. Iyengar, J. J. Gooding, *Analyst* **2012**, *137*, 829.
[25] N. Wangoo, J. Kaushal, K. Bhasin, S. Mehta, C. R. Suri, *Chem. Commun.* **2010**, *46*, 5755.
[26] J.-M. Moon, D.-M. Kim, M. H. Kim, J.-Y. Han, D.-K. Jung, Y.-B. Shim, *Biosens. Bioelectron.* **2017**, *91*, 128.
[27] Y. Boonyasit, W. Laiwattanapaisal, O. Chailapakul, J. Emnéus, A. R. Heiskanen, *Anal. Chem.* **2016**, *88*, 9582.
[28] S. Liu, U. Wollenberger, M. Katterle, F. W. Scheller, *Sens. Actuators, B* **2006**, *113*, 623.
[29] Y. Zhou, H. Dong, L. Liu, Y. Hao, Z. Chang, M. Xu, *Biosens. Bioelectron.* **2015**, *64*, 442.
[30] M. Syamala Kiran, T. Itoh, K.-i. Yoshida, N. Kawashima, V. Biju, M. Ishikawa, *Anal. Chem.* **2010**, *82*, 1342.
[31] I. Barman, N. C. Dingari, J. W. Kang, G. L. Horowitz, R. R. Dasari, M. S. Feld, *Anal. Chem.* **2012**, *84*, 2474.
[32] S. H. Ang, M. Thevarajah, Y. Alias, S. M. Khor, *Clin. Chim. Acta* **2015**, *439*, 202.
[33] A. K. Mallia, G. T. Hermanson, R. I. Krohn, E. K. Fujimoto, P. K. Smith, *Anal. Lett.* **1981**, *14*, 649.
[34] B. Park, H. G. Park, J.-h. Ji, J. Cho, S. C. Jun, *Micromachines* **2016**, *7*, 136.
[35] S. Y. Kwak, J. K. Yang, S. J. Jeon, H. I. Kim, J. Yim, H. Kang, S. Kyeong, Y. S. Lee, J. H. Kim, *Adv. Funct. Mater.* **2014**, *24*, 5119.
[36] M. Mallya, R. Shenoy, G. Kodyalamoole, M. Biswas, J. Karumathil, S. Kamath, *Photomed. Laser Surg.* **2013**, *31*, 219.
[37] A. Shrivastava, V. Gupta, *Chron. Young Sci.* **2011**, *2*, 21.
[38] S.-J. Jeon, S.-Y. Kwak, D. Yim, J.-M. Ju, J.-H. Kim, *J. Am. Chem. Soc.* **2014**, *136*, 10842.
[39] T. W. Kang, S.-J. Jeon, H.-I. Kim, J. H. Park, D. Yim, H.-R. Lee, J.-M. Ju, M.-J. Kim, J.-H. Kim, *ACS Nano* **2016**, *10*, 5346.
[40] W. G. John, A. Mosca, C. Weykamp, I. Goodall, *Clin. Biochem. Rev.* **2007**, *28*, 163.